Log-Domain Filtering and the Bernoulli Cell

Emmanuel Michael Drakakis, Alison J. Payne, *Member, IEEE*, and Chris Toumazou, *Member, IEEE*

***Abstract*—In this paper, the dynamic behavior of a nonlinear circuit element termed a Bernoulli cell is described, which is composed of a suitably biased bipolar junction transistor (BJT) and an emitter connected grounded capacitor. This cell has application in the synthesis of log-domain filters, since it facilitates the development of a low-level design approach in which a frequency-domain transfer function is decomposed into time-domain current product equalities that can be implemented by direct use of the translinear principle (TLP). Furthermore, the dynamic of a log-domain structure can be analyzed and its frequency response can be easily derived when the embedded Bernoulli cells are identified. An analysis and a synthesis example are presented.**

***Index Terms*—Active filters, analog integrated circuits, translinear circuits.**

I. Introduction

A COMMON feature of both translinear (TL) circuits and log-domain structures is the fact that their operation is based on the large-signal exponential characteristic of bipolar junction transistors (BJT's). TL circuits operate in accordance with the TL principle (TLP), as was elegantly expressed by Gilbert [1]. Generally, TL circuits are not exploited to generate frequency-dependent responses, and real-time static linear and nonlinear functions seem to be their main application area [2], [3]. On the other hand, log-domain filters, an idea originally proposed by Adams [4] and fully articulated by Frey [5], [6], can be considered as comprising suitably interconnected complete TL loops with capacitors placed at loop intersections. This has led to log-domain filters also being classified as dynamic TL circuits [22].

Log-domain filters are a significant class of the exponential state-space (ESS) [6] topologies which have been identified by Tsividis as forming part of a broader branch of structures classified as externally linear internally nonlinear (ELIN) networks [7]. Log-domain filter operation is based on instantaneous companding [8]–[11] and these circuits are of theoretical and technological interest because they potentially offer high-frequency operation, tuneability, and extended dynamic range under low power supply voltages [12]–[15]. Moreover, it has been shown that the exponential characteristic of MOSFET's in weak inversion is particularly suited for log-domain micropower applications [16]. Despite these potential benefits, some crucial performance issues, such as noise behavior and distortion, are still under theoretical and experimental investigation [11], [18]–[20].

Manuscript received January 1, 1997; revised May 1, 1998. This paper was recommended by Associate Editor D. A. Johns.

The authors are with the Department of Electrical and Electronic Engineering, Imperial College, SW7 2BT, London, U.K. (e-mail: a.j.payne@ic.ac.uk).

Publisher Item Identifier S 1057-7122(99)03889-1.

Log-domain filter-synthesis methods proposed so far by Frey [5], [6] and Perry–Roberts [21] start from a high-level transfer function description (either state-space or signal-flow graph) and end up with a circuit-level architecture of integrating nodes interconnected by complete TL loops. The high-level nature of these methods prevents the designer from treating the TL loops as fundamental circuit elements. The state-space synthesis method proposed by Frey is based on an ingenious exponential mapping of the state variables and gives the designer the freedom to choose the particular mapping on any required transfer function. However, the method seems to be difficult to apply for the implementation of filters of a higher order, primarily because it becomes cumbersome for the designer to find and manipulate the large number of state-variable mappings and extract the necessary circuit design equations. The LC-ladder synthesis method proposed by Perry–Roberts is a more modular approach which is suitable for the synthesis of higher order filters, and the resulting circuits are implemented by interconnecting log-domain inverting and noninverting summing integrator blocks. However, a modular approach, although useful, does not seem to provide a more experienced designer with a clear flexibility to investigate new or improved designs. The motivation for this work was thus to attempt to combine at transistor level the modularity of the Perry–Roberts LC-ladder approach with the design freedom of Frey's state-space mapping method.

The analysis of log-domain structures has been addressed by Mulder *et al.* in [22]. The method proposed in [22] is based on the identification of TL loops within the circuit which allows the subsequent elimination of the nonlinear capacitor currents which are treated as unknowns.

In this paper, an alternative bottom-up approach to log-domain filter design is introduced. A simple transistor level cell is identified, composed of a single BJT and an emitter connected grounded capacitor. This cell is shown to obey the nonlinear Bernoulli equation and thus is termed a Bernoulli cell. This provides the designer with an alternative method of evaluating the close connection between the complete TL loops embedded within a log-domain circuit and the resulting dynamic behavior of the circuit. This low-level approach is developed further as a powerful tool for both the analysis and the synthesis of log-domain topologies.

This paper aims to do the following.

1. Describe step by step the derivation of the differential equations that govern a single Bernoulli cell and a cascade of Bernoulli cells.
2. Show the potential of this approach, both as an analysis and as a synthesis tool.
3. Present simulation results that confirm the validity of the proposed approach.

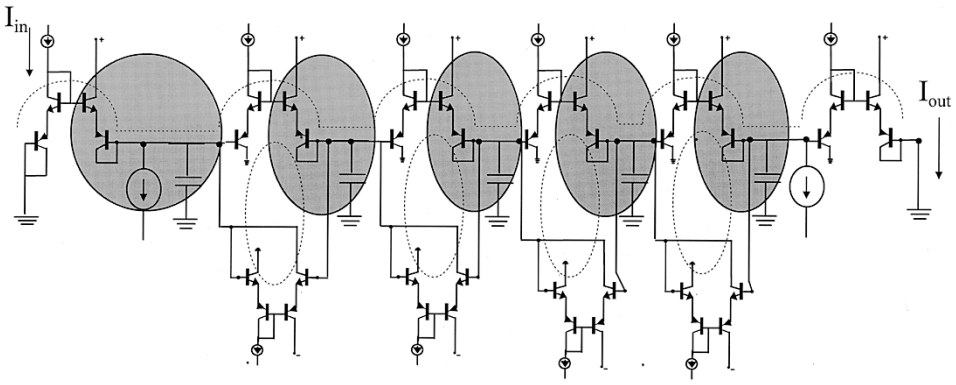

Fig. 1. A fifth-order Chebychev filter: five TL loops are denoted with dotted lines.

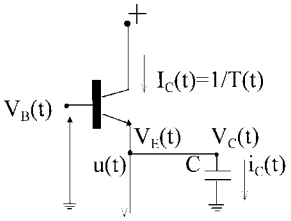

Fig. 2. The Bernoulli cell.

The paper is organized as follows. In Section II the Bernoulli cell is identified. Section III deals with the incorporation of Bernoulli cells in log-domain structures, while Section IV shows the use of the Bernoulli cell as an analysis tool by means of a worked example. Section V develops a low-level log-domain synthesis procedure and describes a design example of a second-order lowpass filter. Section VI presents confirming simulation results for both synthesis and analysis examples, while conclusions are offered in Section VII.

II. The Bernoulli Cell

In general, a high-order log-domain filter could be considered as a system of complete interconnected TL loops with capacitors placed at intersections within the loops (see for example the fifth-order log-domain filter introduced by Perry and Roberts in [21] and shown in Fig. 1). At each intersection a circuit element can be identified, as shown in Fig. 2. This cell is formed by placing a grounded capacitor at the emitter of a forward-biased npn BJT. A complementary version of this cell has been used before by Perry and Roberts (see shaded areas of Fig. 1) whereas the npn-only cell of Fig. 2 itself has been used before by Frey [13] and Punzenberger and Enz [23] for the top-down construction of state-space or integrator-based log-domain filters. Here, the differential equation that governs the BJT collector current of that particular cell is formally identified and is associated with the equations describing the dynamic behavior of log-domain structures in a systematic way. Although the following analysis is presented for an npn-only cell, the treatment of a complementary cell is similar.

Making the reasonable approximation that the BJT collector current $I_C(t)$ (see Fig. 2) obeys the exponential law

$$I_C(t) = Is \exp[(V_B(t) - V_E(t))/V_T] \tag{1}$$

where every term has its usual meaning, then

$$\frac{dV_E(t)}{dt} = \frac{dV_C(t)}{dt} = \dot{V}_C(t) = \frac{i_C(t)}{C} = \frac{[I_C(t) - u(t)]}{C}. \tag{2}$$

Differentiation of (1) yields the following nonlinear differential equation:

$$\dot{I}_C(t) - \left(\frac{\dot{V}_B(t)}{V_T} + \frac{u(t)}{CV_T}\right) I_C(t) + \frac{[I_C(t)]^2}{CV_T} = 0. \tag{3}$$

Interestingly, (3) is of the Bernoulli form and so we will term the circuit of Fig. 2 a Bernoulli cell. Although (3) is nonlinear, it can always be linearized [24]–[27] by means of a nonlinear substitution of the form

$$I_C(t) = 1/T(t), \qquad \text{where } T(t) \neq 0 \tag{4}$$

which transforms (3) into the following:

$$\frac{dT(t)}{dt} + \left(\frac{\dot{V}_B(t)}{V_T} + \frac{u(t)}{CV_T}\right) T(t) - \frac{1}{CV_T} = 0. \tag{5}$$

The terms $\dot{V}_B(t)$ and $u(t)$ are input parameters determinable by the designer, while $T(t)$ is the variable describing the dynamic behavior of the cell. The information provided by $T(t)$ can be accessed indirectly via the Bernoulli-cell collector current since $T(t) = 1/I_C(t)$. One way of accessing $T(t)$ is via the TL principle. For example, when a Bernoulli transistor with collector current $I_C(t)$ forms part of a 2-m emitter junction TL loop, where the k-th junction current is denoted by $I_k(t)$ and all the junctions are considered identical, it holds [1]

$$\prod_{k=1}^{m} I_k(t)(\text{ clockwise}) = \prod_{k=1}^{m} I'_k(t)(\text{anticlockwise}). \tag{6.a}$$

If $I_C(t)$ is the collector current flowing through the jth clockwise junction, then $T(t)$ can be identified as

$$T(t) = \frac{1}{I_C(t)} = \frac{1}{I_j(t)} = \frac{\prod_{k=1}^{m(k\neq j)} I_k(t)(\text{ clockwise})}{\prod_{k=1}^{m} I'_k(t)(\text{ anticlockwise})}. \tag{6.b}$$

Translinear equations of the form [(6.a), (6.b)] are used extensively in later sections of the paper for the analysis and synthesis of log-domain structures.

When viewed in terms of interconnected Bernoulli cells, the key role of TL loops in log-domain structures is clear. The TL loops allow access to the parameter $T(t)$ which linearizes the differential equations controlling the Bernoulli cells' time-domain behavior. In the topology of Fig. 1, five TL loops—illustrated with dotted lines—can be identified, which access the dynamic behavior of the five complementary Bernoulli cells.

III. Bernoulli Cells in Log-Domain Structures

A. A Single Input-Driven Bernoulli Cell

A convenient way of applying the Bernoulli cell of Fig. 2 to log-domain filtering is shown in Fig. 3(a). The input current $I_{\mathbf{in}}(t)$ is converted to a logarithmically compressed voltage $V_B(t)$ where

$$\dot{V}_B(t) = V_T \frac{\dot{I}_{\mathbf{in}}(t)}{I_{\mathbf{in}}(t)} = V_T \frac{d}{dt}\{\ln[I_{\mathbf{in}}(t)]\}. \quad (7)$$

Substitution of (7) into (5) yields

$$CV_T \frac{d}{dt}\{\ln[T(t)I_{\mathbf{in}}(t)]\} + u(t) = \frac{1}{T(t)} = I_C(t). \quad (8)$$

Equation (8) can be interpreted as a transformed expression for KCL at the emitter of the Bernoulli-cell BJT. Recall that $I_C(t)$ is the collector current whereas $u(t)$ is the current sourced from the transistor emitter. Thus, the capacitor current is given by

$$i_C(t) = CV_T \frac{d}{dt}\{\ln[T(t)I_{\mathbf{in}}(t)]\}. \quad (9)$$

Obviously, this is not the only way of driving a Bernoulli cell. Any topology which ensures that the base terminal variations $\dot{V}_B(t)$ shown in Fig. 2 are equal to the quantity $V_T d/dt\{\ln[I_{\mathbf{in}}(t)]\} = V_T \frac{\dot{I}_{\mathbf{in}}(t)}{I_{\mathbf{in}}(t)}$, where $I_{\mathbf{in}}(t)$ is the input signal, will realize the transformed KCL expression of (8).

B. Interconnection of Bernoulli Cells

In Fig. 3(b) two Bernoulli cells are connected via a level shifter Q_{01} (evidently this is not the only possible way of interconnecting two Bernoulli cells, but this interconnection allows operation at low power supply voltages). The differential equations describing the two interconnected Bernoulli cells can be derived as follows. For the first cell [see Fig. 3(b)] it has already been shown

$$C_1 V_T \frac{d}{dt}\{\ln[T_1(t)I_{\mathbf{in}}(t)]\} + u_1(t) = \frac{1}{T_1(t)} = I_{C_1}(t). \quad (10)$$

The linearized expression for the second cell can be derived from (5) by substituting $I_{C_2}(t) = 1/T_2(t)$

$$\frac{dT_2(t)}{dt} + \left(\frac{\dot{V}_{B_2}(t)}{V_T} + \frac{u_2(t)}{CV_T}\right) T_2(t) - \frac{1}{C_2 V_T} = 0. \quad (11)$$

From (9) is clear that (see Fig. 3(b))

$$\frac{dV_{C_1}(t)}{dt} = V_T \frac{d}{dt}\{\ln[T_1(t)I_{\mathbf{in}}(t)]\}. \quad (12)$$

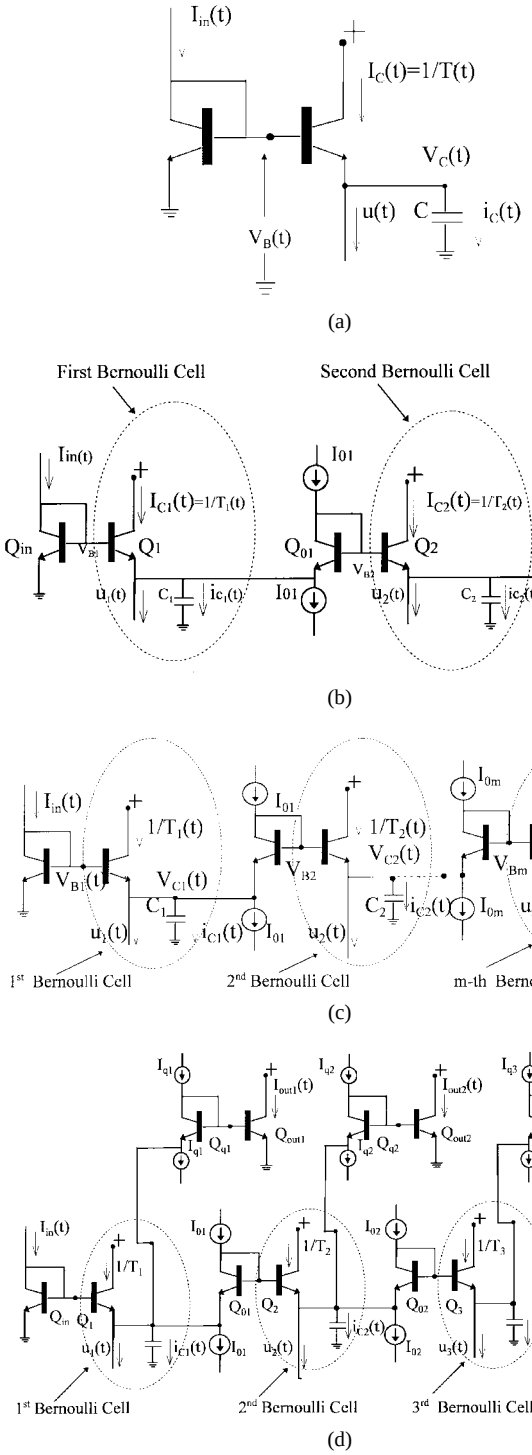

Fig. 3(a). A logarithmically driven Bernoulli cell. (b) Two Bernoulli cells interconnected via level shifter I_{01}. (c) m Bernoulli cells interconnected by level-shifters. (d) The output currents $I_{\mathrm{out}\,k}$ sense the variables $w_k(t)$.

Since the level shifter Q_{01} ensures that $V_{B2}(t) = V_{C_1}(t) + V_T \ln(I_{01}/I_S) \Rightarrow \dot{V}_{B_2}(t) = \dot{V}_{C_1}(t)$, I_{01} being a constant current source, (11) finally yields

$$C_2 V_T \frac{d}{dt}\{\ln[T_2(t)T_1(t)I_{\mathbf{in}}(t)]\} + u_2(t) = \frac{1}{T_2(t)} = I_{C2}(t). \quad (13)$$

The generalization of (13) for the last cell of m Bernoulli cells, interconnected as shown in Fig. 3(c), when $dV_{Bn}(t)/dt = dV_{C_{n-1}}(t)/dt (n = 2, \ldots, m)$ is given by

$$C_m V_T \frac{d}{dt}\{\ln[T_m(t)T_{m-1}(t)\cdots T_1(t)I_{\text{in}}(t)]\} + u_m(t) = \frac{1}{T_m(t)} = I_{C_m}(t). \tag{14}$$

Equations (10), (13) and (14) are a set of transformed KCL equations applied at the emitters of the first, second, and mth cells, respectively. The respective Bernoulli-cell capacitor currents can thus be stated as

$$\begin{aligned} i_{C_1}(t) &= C_1 V_T \frac{d}{dt}\{\ln[T_1(t)I_{\text{in}}(t)]\} \\ i_{C_2}(t) &= C_2 V_T \frac{d}{dt}\{\ln[T_2(t)T_1(t)I_{\text{in}}(t)]\} \\ &\cdots \\ i_{C_m}(t) &= C_m V_T \frac{d}{dt}\{\ln[T_m(t)\cdots T_2(t)T_1(t)I_{\text{in}}(t)]\} \\ &= C_m V_T \frac{d}{dt}\left\{\ln\left(\left[\prod_{k=1}^{m} T_k(t)\right] I_{\text{in}}(t)\right)\right\}. \end{aligned} \tag{15.a}$$

Substituting the positive product terms for a new variable $w_k(t)$, i.e.,

$$w_k(t) = \left(\prod_{j=1}^{k} T_j(t)\right) I_{\text{in}}(t) = T_k(t) w_{k-1}(t) \tag{15.b}$$

(15.a) takes the form

$$\begin{aligned} i_{C_1}(t) &= C_1 V_T \frac{d}{dt}\{\ln[w_1(t)]\} \\ i_{C_2}(t) &= C_2 V_T \frac{d}{dt}\{\ln[w_2(t)]\} \\ &\cdots \\ i_{C_m}(t) &= C_m V_T \frac{d}{dt}\{\ln[w_m(t)]\}. \end{aligned} \tag{15.c}$$

From (15.c) it can be concluded that

$$\begin{aligned} w_1(t) &= \mu_1 \exp\left[\frac{V_{C_1}(t)}{V_T}\right] \\ w_2(t) &= \mu_2 \exp\left[\frac{V_{C_2}(t)}{V_T}\right] \\ &\cdots \\ w_m(t) &= \mu_m \exp\left[\frac{V_{C_m}(t)}{V_T}\right] \end{aligned} \tag{15.d}$$

where $\mu_1, \mu_2, \ldots, \mu_m$ are constant in time quantities and $V_{Cn}(t)$ are the respective nth cell capacitor voltages. The $w_k(t)$ variables are directly related to the Bernoulli-cell collector currents since $w_k(t) = I_{\text{in}}(t)/[I_{C_1}(t)\cdots I_{C_k}(t)]$, with $I_{C_j}(t)$ being the respective jth Bernoulli-cell collector current. Note that the $w(t)$ variables in (15.d) are essentially the exponential mappings defined by Frey [5], although Frey's state-space synthesis method requires the quantities μ_1 etc., to be selected (arbitrarily) at the mapping stage. In this case, the quantities remain presently undefined.

Substitution of the $w_k(t)$ variables given by (15.b) allows the transformed KCL (10), (13) and (14) to be reexpressed as

$$\begin{aligned} C_1 V_T \dot{w}_1(t) + u_1(t) w_1(t) &= I_{\text{in}}(t) \\ C_2 V_T \dot{w}_2(t) + u_2(t) w_2(t) &= w_1(t) \\ &\cdots \\ C_m V_T \dot{w}_m(t) + u_m(t) w_m(t) &= w_{m-1}(t). \end{aligned} \tag{16}$$

This system of linear ordinary differential equations describes the dynamic behavior of the m interconnected Bernoulli cells. These interconnected cells can be considered as the basic backbone of the log-domain filter. The dimensional consistency of (16) can be readily verified. The variables $w_k(t)$ can be sensed by means of additional pairs of transistors such as $Q_{q2}Q_{\text{out}2}$ and $Q_{q3}Q_{\text{out}3}$, shown in Fig. 3(d). By applying the TLP to the loop $Q_{\text{in}}Q_1Q_{01}Q_2Q_{q2}Q_{\text{out}2}$

$$I_{\text{in}}(t)I_{01}I_{q2} = \frac{1}{T_1(t)}\frac{1}{T_2(t)} I_{\text{out}2}(t) \Rightarrow I_{\text{out}2}(t) = I_{q2}I_{01}[T_2(t)T_1(t)I_{\text{in}}(t)] = I_{q2}I_{01}w_2(t). \tag{17.a}$$

Similarly, for the loop $Q_{\text{in}}Q_1Q_{01}Q_2Q_{02}Q_3Q_{q3}Q_{\text{out}3}$

$$\begin{aligned} I_{\text{out}3}(t) &= I_{01}I_{02}I_{q3}[T_3(t)T_2(t)T_1(t)I_{\text{in}}(t)] \\ &= I_{01}I_{02}I_{q3}w_3(t). \end{aligned} \tag{17.b}$$

Generalizing this expression for the m-th Bernoulli cell

$$I_{\text{out}m}(t) = I_{01}I_{02}\cdots I_{qm}w_m(t) = \left(\prod_{k=1}^{m-1} I_{ok}\right) I_{qm}w_m(t). \tag{17.c}$$

The application of Bernoulli cells to log-domain filtering, either as an analysis tool or as a synthesis tool, is based on the appropriate interpretation of (10), (13) and (14) or the equivalent system of (16). Equations (16) could be considered as a modular "log-domain state-space," with the quantities $w_k(t)$ representing the state-variables, and can be used for the synthesis of log-domain filters by equating them to a conventional linear state-space description of a desired transfer function [28], [29].

This paper focuses on presenting an alternative low-level synthesis route,other than that described in [28], [29], and also describes the use of (16) as an analysis tool. In the following section an analysis example is presented in order to familiarize the reader with the proposed approach.

IV. Bernoulli-Cell-Based Analysis of Log-Domain Structures

The analysis of log-domain structures is fairly simple if an interconnection of Bernoulli cells can be identified since the dynamic behavior of the cells can be described by (16) which, as was previously shown, correspond to KCL expressions at the emitters of the Bernoulli-cell transistors. When the

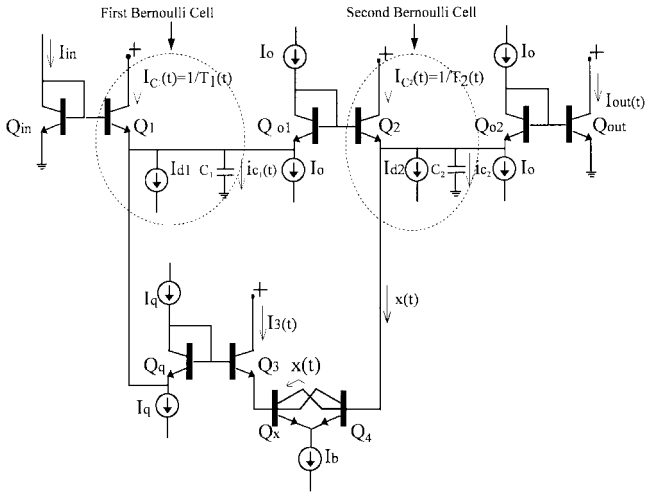

Fig. 4. Bernoulli-cell analysis example.

following steps are taken, a given log-domain structure can be analyzed in a systematic way.

i. Identify the interconnected Bernoulli cells and express the time-domain relations governing their dynamic behavior in terms of the variables $w_k(t)$ (or equivalently of the collector currents $1/T_k(t)$). For a translinear topology this procedure is straightforward since the TLP can be applied directly to determine the required time-domain current-product equalities.

ii. Apply the expressions for the $w_k(t)$ variables found during step i. to the system of differential equations described by (16). When the resulting differential equation(s) describing the relation between the input and the output(s) are linear with constant coefficients, the input–output behavior in the frequency domain can be derived by applying the Laplace Transform.

The above procedure is best clarified by means of an example. Consider the log-domain structure shown in Fig. 4 which is obtained from the basic backbone shown in Fig. 3(b) by subtracting a current $x(t)$ from the second cell integration node and adding two current sources I_{d1} and I_{d2} to the first and second cell capacitor nodes, respectively. The topology can be interpreted as two Bernoulli cells interconnected by means of two TL loops: one formed by transistors $Q_{\rm in}Q_1Q_{01}Q_2Q_{02}Q_{\rm out}$ (first TL loop) and the second by transistors $Q_{01}Q_2Q_4Q_xQ_3Q_q$ (second TL loop). Applying the TLP to these loops, neglecting base currents and series ohmic resistances (step i)

first TL loop

$$\begin{aligned} I_{\rm in}(t)I_0I_0 &= I_{C_1}(t)I_{C_2}(t)I_{\rm out}(t) \Rightarrow \\ I_{\rm in}(t)\frac{1}{I_{C_1}(t)}\frac{1}{I_{C_2}(t)}I_0^2 &= I_{\rm out}(t) \Rightarrow \\ [I_{\rm in}(t)T_1(t)T_2(t)]I_0^2 &= I_{\rm out}(t) \Rightarrow \\ I_{\rm out}(t) &= I_0^2 w_2(t) \end{aligned} \tag{18.a}$$

second TL loop

$$\begin{aligned} I_0I_3(t)x(t) &= I_{C_2}(t)I_3(t)I_q \Rightarrow \\ x(t)\frac{1}{I_{C_2}(t)} &= \frac{I_q}{I_0} \Rightarrow \\ x(t)T_2(t)[T_1(t)I_{\rm in}(t)] &= \frac{I_q}{I_0}[T_1(t)I_{\rm in}(t)] \Rightarrow \\ x(t)w_2(t) &= \frac{I_q}{I_0}w_1(t). \end{aligned} \tag{18.b}$$

Proceeding to step ii. and realizing that $u_1(t) = I_{d1}$ and $u_2(t) = I_{d2} + x(t)$, it will hold from (16) (for simplicity identical capacitors $C_1 = C_2 = C$ are assumed)

$$\begin{aligned} CV_T\dot{w}_1(t) + I_{d1}w_1(t) &= I_{\rm in}(t) \\ CV_T\dot{w}_2(t) + [I_{d2} + x(t)]w_2(t) &= w_1(t). \end{aligned} \tag{19}$$

From (18.b) $x(t)w_2(t) = [I_q/I_0]w_1(t)$, thus the second differential equation is linear with constant in time coefficients. Applying the Laplace transform to the above system (19) of differential equations produces (the steady state response is considered)

$$\begin{aligned} CV_TsW_1(s) + I_{d1}W_1(s) &= I_{\rm in}(s) \\ CV_TsW_2(s) + I_{d2}W_2(s) + \frac{I_q}{I_0}W_1(s) &= W_1(s) \\ I_{\rm out}(s) &= I_0^2W_2(s) \end{aligned} \tag{20}$$

where the third equation is obtained from (18.a) since $I_{\rm out}(t) = I_0^2 w_2(t)$.

Elementary algebra can now be used to solve for the quantity $W_2(s)$ and show that the input–output relation in frequency domain is given by

$$\frac{I_{\rm out}(s)}{I_{\rm in}(s)} = \frac{I_0(I_0 - I_q)/(CV_T)^2}{s^2 + \frac{I_{d1}+I_{d2}}{CV_T}s + \frac{I_{d1}I_{d2}}{(CV_T)^2}} \tag{21}$$

which corresponds to a lowpass behavior with a pole frequency equal to

$$\omega_0 = \frac{\sqrt{I_{d1}I_{d2}}}{CV_T} \tag{22}$$

and a quality factor

$$Q = \frac{\sqrt{I_{d1}I_{d2}}}{I_{d1} + I_{d2}}. \tag{23}$$

The gain factor of the filter is given by

$$K_g = I_0(I_0 - I_q)/(I_{d1}I_{d2}). \tag{24}$$

V. Bernoulli-Cell-Based Synthesis of Log-Domain Filters

This section discusses various synthesis issues for a second-order lowpass biquad, leading to the proposal of a low-level bottom-up synthesis procedure. The first two equations provided by (16) which, for convenience, are repeated below describe the dynamic behavior of the two interconnected Bernoulli cells of Fig. 3(b)

$$C_1V_T\dot{w}_1(t) + u_1(t)w_1(t) = I_{\rm in}(t) \tag{25.a}$$

$$C_2V_T\dot{w}_2(t) + u_2(t)w_2(t) = w_1(t). \tag{25.b}$$

By taking their Laplace transform (considering steady-state behavior only)

$$C_1V_T sW_1(s) + L\{u_1(t)w_1(t)\} = I_{\text{in}}(s) \quad (26.a)$$
$$C_2V_T sW_2(s) + L\{u_2(t)w_2(t)\} = W_1(s). \quad (26.b)$$

(The symbol L denotes the application of the Laplace transform).

Substituting (26.b) into (26.a) yields

$$C_1C_2V_T^2s^2W_2(s) + (C_1V_Ts)\,L\{u_2(t)w_2(t)\} + L\{u_1(t)w_1(t)\} = I_{\text{in}}(s). \quad (27)$$

The $w_2(t)$ (or $W_2(s)$) variable can be sensed by means of an additional pair of BJT's, as discussed earlier in Section III. Referring to Fig. 3(d), for the output current $I_{\text{out}2}(t)$ (which for convenience is hereafter simply denoted as $I_{\text{out}}(t)$) it will hold

$$I_{\text{out}}(t) = I_{01}I_{q2}w_2(t) \quad (28)$$

or taking the Laplace transform

$$I_{\text{out}}(s) = I_{01}I_{q2}W_2(s). \quad (29)$$

Equation (29) reveals that when the quantity $W_2(s)$ is a second-order lowpass filtered version of the input $I_{\text{in}}(s)$, then the transfer function $I_{\text{out}}(s)/I_{\text{in}}(s)$ will correspond to a second-order lowpass filter. From (27), when

$$L\{u_2(t)w_2(t)\} = k_2\,W_2(s) \quad (30.a)$$

and

$$L\{u_1(t)w_1(t)\} = k_1\,W_2(s) \quad (30.b)$$

with k_2, k_1 real positive constants, it will hold

$$\frac{W_2(s)}{I_{\text{in}}(s)} = \frac{1}{C_1C_2V_T^2s^2 + (k_2C_1V_T)s + k_1}. \quad (31)$$

Thus, when (30.a) and (30.b) hold, the combination of (29) and (31) gives

$$\frac{I_{\text{out}}(s)}{I_{\text{in}}(s)} = \frac{I_{01}I_{q2}}{C_1C_2V_T^2s^2 + (k_2C_1V_T)s + k_1} \quad (32)$$

which corresponds to the transfer function of a second-order lowpass filter.

In order for the desired transfer function to be realized by means of a cascade of two Bernoulli cells, the necessary conditions (30.a) and (30.b) should be satisfied and the output current $I_{\text{out}}(t)$ should be proportional to the variable $w_2(t)$.

In what follows it will be shown that when a certain set of substitutions is applied to the time-domain equivalent of (32) and a subsequent continued fraction expansion is adopted, then the conditions (30.a) and (30.b) necessary for the realization of (32) can be extracted. More specifically, to understand how (32) can be synthesized, note that it can be written equivalently as

$$C_1C_2V_T^2s^2I_{\text{out}}(s) + (k_2C_1V_T)sI_{\text{out}}(s) + k_1I_{\text{out}}(s) = I_{01}I_{q2}I_{\text{in}}(s) \quad (33)$$

and applying the inverse Laplace transform to (33) yields

$$C_1C_2V_T^2\ddot{I}_{\text{out}}(t) + (k_2C_1V_T)\dot{I}_{\text{out}}(t) + k_1I_{\text{out}}(t) = I_{01}I_{q2}I_{\text{in}}(t) \quad (34.a)$$

or

$$\frac{I_{\text{out}}(t)}{I_{\text{in}}(t)} = \frac{I_{01}I_{q2}}{C_1C_2V_T^2\frac{\ddot{I}_{\text{out}}(t)}{I_{\text{out}}(t)} + (k_2C_1V_T)\frac{\dot{I}_{\text{out}}(t)}{I_{\text{out}}(t)} + k_1}. \quad (34.b)$$

Since

$$\frac{\dot{I}_{\text{out}}(t)}{I_{\text{out}}(t)} = \frac{d}{dt}\{\ln|I_{\text{out}}(t)|\}$$

and

$$\frac{\ddot{I}_{\text{out}}(t)}{I_{\text{out}}(t)} = \frac{\ddot{I}_{\text{out}}(t)}{\dot{I}_{\text{out}}(t)}\frac{\dot{I}_{\text{out}}(t)}{I_{\text{out}}(t)} = \frac{d}{dt}\{\ln|\dot{I}_{\text{out}}(t)|\}\frac{d}{dt}\{\ln|I_{\text{out}}(t)|\}$$

(34.b) can be expressed as (35) at the bottom of this page. Equation (35) is the time-domain equivalent of (32).

At this point, recall from (15.c) that the mth Bernoulli-cell capacitor current has the form

$$i_{C_m}(t) = C_mV_T\frac{d}{dt}\{\ln[w_m(t)]\}.$$

This suggests that (35) can be physically implemented by substituting Bernoulli-cell capacitor currents for terms of the form $d/dt\{\ln[]\}$.

The question arises as to which capacitor current should be chosen as the substitute for each of the separate terms $d/dt\{\ln|I_{\text{out}}(t)|\}$ and $d/dt\{\ln|\dot{I}_{\text{out}}(t)|\}$. At the circuit level there will be two Bernoulli-cell capacitor currents, $i_{C_1}(t)$ and $i_{C_2}(t)$, so there are two different possible substitutions and the number of possible substitutions will clearly increase for a higher order filter. In order to decide which substitutions to choose we must ask which of the resulting design equations will be physically realizable and will correspond to the desired transfer functions. However, let us put this question aside for the moment and simply choose to substitute $d/dt\{\ln|I_{\text{out}}(t)|\} \rightarrow i_{C_1}(t)/C_1V_T$ and $d/dt\{\ln|\dot{I}_{\text{out}}(t)|\} \rightarrow i_{C_2}(t)/C_2V_T$.

Equation (35) then becomes

$$\frac{I_{\text{out}}(t)}{I_{\text{in}}(t)} = \frac{I_{01}I_{q2}}{i_{C_1}(t)i_{C_2}(t) + k_2i_{C_1}(t) + k_1}. \quad (36)$$

At this point it is important to underline that the input–output relation as expressed by (36) is identical to the one obtained

$$\frac{I_{\text{out}}(t)}{I_{\text{in}}(t)} = \frac{I_{01}I_{q2}}{C_1C_2V_T^2\frac{d}{dt}\{\ln|I_{\text{out}}(t)|\}\frac{d}{dt}\{\ln|\dot{I}_{\text{out}}(t)|\} + (k_2C_1V_T)\frac{d}{dt}\{\ln|I_{\text{out}}(t)|\} + k_1}. \quad (35)$$

when the time-domain relations imposed by (28), (30.a), and (30.b) in conjunction with (25.a) and (25.b) are taken into consideration (due to a lack of space the respective simple calculations are not shown). Hence, the proposed substitutions ensure that the time-domain input–output relation is correctly expressed when the frequency-domain response is a lowpass biquad. Once this is achieved the expression (36) can be implemented by isolating quantities of the form $i_{C_m}(t) + u_m(t)$ which will represent Bernoulli-cell collector currents $I_{C_m}(t) = 1/T_m(t)$. This can be done via a continued fraction decomposition

$$\frac{I_{\text{out}}(t)}{I_{\text{in}}(t)} = \frac{\frac{I_{01}I_{q2}}{i_{C_2}(t)+k_2}}{i_{C_1}(t) + \frac{k_1}{i_{C_2}(t)+k_2}}. \tag{37}$$

Equation (37) provides all the necessary information to implement the required transfer function, Terms of the form $i_{C_m}(t) + u_m(t)$ can be identified where

$$u_2(t) = k_2 \tag{38.a}$$

$$u_1(t) = \frac{k_1}{i_{C_2}(t) + u_2(t)}. \tag{38.b}$$

Observe that when (38.a) and (38.b) hold, (30.a) and (30.b) which ensure the realization of the desired transfer function are fulfilled. The multiplication of (38.a) by the variable $w_2(t)$ and the application of the Laplace transform leads to (30.a). Similarly, recalling that $1/i_{c_2}(t) + u_2(t) = T_2(t) = w_2(t)/w_1(t)$ [from (15.b)] and expressing (38.b) as $u,(t), w_1(t) = k_1 w_2(t)$ leads to (30.b) when the Laplace transform is applied.

Equation (37) can also be written as

$$\frac{I_{\text{out}}(t)}{I_{\text{in}}(t)} = \frac{I_a(t)}{i_{C_1}(t) + u_1(t)} \tag{39}$$

where

$$I_a(t) = \frac{I_{01}I_{q2}}{i_{C_2}(t) + u_2(t)}. \tag{40}$$

Equations (39) and (40) correspond to products of currents and it will be shown that they can be simply implemented using translinear loops. This method of capacitor current substitution and continued fraction expansion can be extended to higher order filters in a fairly straightforward way. For higher order filters however, the earlier question of which capacitor current substitution to choose becomes more important, since certain choices of substitution will result in design equations which are difficult to implement or nonrealizable. To ensure that a physically realizable set of design equations that correspond to the desired frequency-domain behavior is always obtained, the following substitution should always be chosen:

$$\frac{d}{dt}\left\{\ln\left|\frac{d^n}{dt^n}I_{\text{out}}(t)\right|\right\} \rightarrow \frac{i_{C_{n+1}}(t)}{C_{n+1}V_T}$$

with $i_{C_{n+1}}(t)$ being the $(n+1)$-th Bernoulli-cell capacitor current.

For the case of higher order all-pole behaviors governed by internal conditions of the form (30.a) and (30.b), an analytical treatment similar to the one corresponding to (25.a)–(36) would again reveal that the above substitutions ensure that the time domain input–output relation is equivalent to the required frequency domain response.

Equation (35), and similar expressions for higher order filters, do not take into consideration the internal dynamics of the structure. They are simply derived by means of the rearrangement of the differential equation corresponding to the desired external behavior of the system. Clearly, a common (internally) linear system could just as easily correspond to the same differential equation. The realization that (35), or similar ones for higher order behaviors, ignores the internal dynamics of the structure, means that it would be pointless to examine whether quantities of the form $d/dt\{\ln||\}$ equal $i_{c_j}(t)/C_jV_\tau$. In fact, the internal capacitor currents are described, in general, by rather complicated expressions of the output current and its derivatives and not by elegant expressions of the form $d/dt\{\ln|I_{\text{out}}(t)|\}, d/dt\{\ln|\dot{I}_{\text{out}}(t)|\}, d/dt\{\ln|\ddot{I}_{\text{out}}(t)|\}$, etc.

On the other hand, as long as the suggested substitutions take place, it is ensured that the input–output relation in the time domain is equivalent to the desired frequency domain response [recall (36) and the comments there].

Hence, it is for the above reasons that the symbol $\rightarrow$ instead of the more common $=$ has been adopted for the proposed substitutions.

If the desired transfer function contains zeros, the time-domain equivalent of the desired transfer function will incorporate terms of the form $d/dt\{\ln|d^n/dt^n I_{\text{in}}(t)|\}$ in the numerator. The appropriate substitutions can be found by means of a similar analytic treatment and (due to a lack of space) will be discussed elsewhere.

Before clarifying the synthesis procedure with a specific example, the proposed all-pole transfer function synthesis steps are summarized below:

i) Convert the frequency domain transfer function to its time-domain equivalent by applying the inverse Laplace transform.
ii) Substitute the terms of the form $d/dt\{\ln|d^n/dt^n I_{\text{out}}(t)|\}$ with the quantity $i_{C_{n+1}}(t)/C_{n+1}V_T$, with $i_{C_{n+1}}(t)$ being the $(n+1)$-th Bernoulli-cell capacitor current.
iii) Extract the necessary design equations in the form of time-domain current product equalities, by expressing the time-domain equivalent of the desired transfer function in continued fractions form,
iv) Implement the necessary TL design equations; the designer is left with the freedom to choose any appropriate (translinear or not) architecture which satisfies the required TL design equations, although a translinear-only design strategy seems to facilitate the design.

The proposed bottom-up synthesis procedure is best clarified by an example; consider the case of a second order lowpass filter synthesis with a transfer function given by

$$\frac{I_{\text{out}}(s)}{I_{\text{in}}(s)} = \frac{b}{s^2 + as + b} = \frac{\omega_o^2}{s^2 + \left(\frac{\omega_o}{Q}\right)s + \omega_o^2} \tag{41.a}$$

or, in time-domain (step i)

$$\ddot{I}_{\text{out}}(t) + a\dot{I}_{\text{out}}(t) + bI_{\text{out}}(t) = bI_{\text{in}}(t) \tag{41.b}$$

since $[\dot{I}_{\rm out}(t)/I_{\rm out}(t)] = d\{\ln|I_{\rm out}(t)|\}/dt$ and $[\ddot{I}_{\rm out}(t)/\dot{I}_{\rm out}(t)] = d\{\ln|\dot{I}_{\rm out}(t)|\}/dt$, (41.b) can be rewritten

$$\frac{I_{\rm out}(t)}{I_{\rm in}(t)} = \frac{b}{b + \{a\frac{d}{dt}[\ln|I_{\rm out}|]\} + \{\frac{d}{dt}[\ln|I_{\rm out}|]\}\{\frac{d}{dt}[\ln|\dot{I}_{\rm out}|]\}}. \tag{42}$$

Replacing terms of the form $d/dt\{\ln|d^n/dt^n I_{\rm out}(t)|\}$ with the $(n+1)$th Bernoulli-cell capacitor currents $i_{C_{n+1}}(t)/C_{n+1}V_T$ (step ii), i.e., $d/dt\{\ln[I_{\rm out}(t)]\} \rightarrow i_{C_1}(t)/C_1V_T$ and $d/dt\{\ln|\dot{I}_{\rm out}(t)|\} \rightarrow i_{C_2}(t)/C_2V_T$, (42) reduces to

$$\frac{I_{\rm out}(t)}{I_{\rm in}(t)} = \frac{bC_1C_2V_T^2}{bC_1C_2V_T^2 + aC_2V_T i_{C_1}(t) + i_{C_1}(t)i_{C_2}(t)}. \tag{43}$$

Equation (43) can be expressed in continued fractions form

$$\frac{I_{\rm out}(t)}{I_{\rm in}(t)} = \frac{\frac{bC_1C_2V_T^2}{i_{C_2}(t)+(aC_2V_T)}}{i_{C_1}(t) + \frac{bC_1C_2V_T^2}{i_{C_2}(t)+(aC_2V_T)}}. \tag{44}$$

As was previously explained, the purpose of rearranging (43) into continued fractions form is to create and isolate terms of the form $i_{C_m}(t) + u_m(t)$ to identify both the $u_m(t)$ currents and the conditions which are necessary for the generation of the desired transfer function.

From (44) it follows that

$$u_2(t) = aC_2V_T \tag{45.a}$$

(since the quantity aC_2V_T is associated with the capacitor current $i_{C_2}(t)$) and

$$u_1(t) = \frac{bC_1C_2V_T^2}{i_{C_2}(t) + (aC_2V_T)} = y(t) \tag{45.b}$$

(since $y(t)$ is associated with the current $i_{C_1}(t)$).

$y(t)$ represents a necessary current sourced from the emitter of the first Bernoulli cell. The identification of the current $u_1(t) = y(t)$ allows the decomposition of (44) into the following relations:

$$\frac{bC_1C_2V_T^2}{i_{C_2}(t) + (aC_2V_T)} = y(t) \tag{46.a}$$

and

$$\frac{I_{\rm out}(t)}{I_{\rm in}(t)} = \frac{y(t)}{i_{C_1}(t) + y(t)}. \tag{46.b}$$

[compare with (38.b), (39), and (40)].

From (41) is clear that the dimension of quantities $bC_1C_2V_T^2$ and aC_2V_T are $[A]^2$ and $[A]$, respectively. The relations (46.a) and (46.b) correspond to time-domain current product equalities, and thus reveal the necessary TL design constraints. It should now be clear how the recursive form of continued fractions can be used to derive these constraints (step iii).

Proceeding to step (iv), the designer already knows the backbone [shown in Fig. 3(b)] of the final topology (shown in Fig. 5) since two Bernoulli-cell capacitor currents are

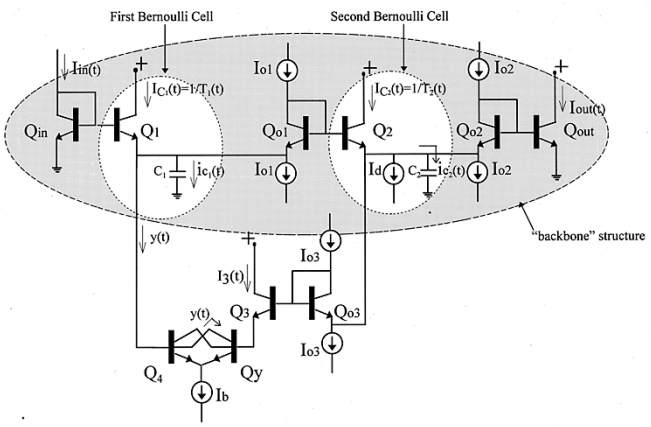

Fig. 5. Bernoulli-cell synthesis example.

needed for the desired frequency response to be realized. Rearrangement of (46.a) and (46.b) yields

$$\begin{aligned} I_{\rm out}(t)\big[i_{C_1}(t) + y(t)\big] &= I_{\rm in}(t)y(t) \\ y(t)\big[i_{C_2}(t) + aC_2V_T\big] &= bC_1C_2V_T^2 \end{aligned}. \tag{47.a}$$

Rearranging terms

$$\begin{aligned} I_{\rm out}(t)\big[i_{C_1}(t) + y(t)\big]\big[i_{C_2}(t) + aC_2V_T\big] &= bC_1C_2V_T^2 I_{\rm in}(t) \\ y(t)\big[i_{C_2}(t) + aC_2V_T\big] &= bC_1C_2V_T^2 \end{aligned}. \tag{47.b}$$

Since $I_{C_1}(t) = i_{C_1}(t) + y(t)$ and $I_{C_2}(t) = i_{C_2}(t) + aC_2V_T$

$$I_{\rm out}(t)I_{C_1}(t)I_{C_2}(t) = bC_1C_2V_T^2 I_{\rm in}(t) \tag{48.a}$$

$$y(t)I_{C_2}(t) = bC_1C_2V_T^2. \tag{48.b}$$

Equation (48.a) describes the operation of the backbone structure shown in Fig. 3(b) when an extra level shifter and an output BJT are added [compare with Figs. 3(d) and (5)]. Applying the TLP to the loop formed by $Q_{\rm in}Q_1Q_{01}Q_2Q_{02}Q_{\rm out}$ in Fig. 5:

$$I_{\rm out}I_{C_1}(t)I_{C_2}(t) = I_{01}I_{02}I_{\rm in}(t). \tag{49}$$

Comparing the necessary (48.a) with (49), which corresponds to a circuit-level implementation, reveals the condition

$$bC_1C_2V_T^2 = I_{01}I_{02}. \tag{50}$$

The next step is to design the additional circuitry which will implement (48.b) and which will finally define the desired collector currents $I_{C_1}(t)$ and $I_{C_2}(t)$. Since $I_{C_2}(t) = i_{C_2}(t) + aC_2V_T$ where aC_2V_T is a constant term with dimensions of $[A]$, a constant current source I_d is added at this node, i.e.,

$$u_2(t) = aC_2V_T = I_d. \tag{51}$$

The block shown in Fig. 6 [12], [13], [30] can be used to implement the constraint (48.b), since by connecting terminals A and B at the emitters of Q_1 and Q_2, respectively, (see Fig. 5) and applying the TLP to the loop formed by

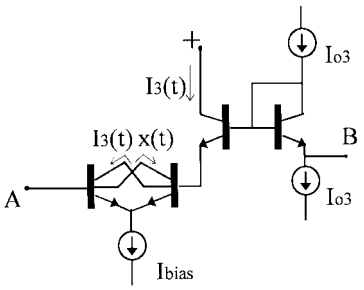

Fig. 6. Auxiliary TL circuitry.

$Q_{01}Q_4Q_yQ_3Q_{03}Q_2$ the following relation is obtained:

$$I_{C_2}(t)I_3(t)y(t) = I_{01}I_3(t)I_{03}. \tag{52}$$

Equation (52) implements equality (48.b) when

$$I_{01}I_{03} = bC_1C_2V_T^2. \tag{53}$$

Any other circuitry which implements (48.b) could be used to realize the same transfer function.

According to (50) and (53) $I_{02} = I_{03}$: a convenient setting is $I_{01} = I_{02} = I_{03} = \sqrt{b}\sqrt{C_1C_2}V_T$. Note that there is no indication as to the value of I_b (see Fig. 5), although clearly $I_b = I_3(t) + y(t)$ at any instant when the TL loop is suitably biased. From (41), (50) and (51) it can be derived that $\omega_0^2 = I_{01}I_{02}/(C_1C_2V_T^2)$ and $(\omega_0/Q) = I_d/(C_2V_T)$ Thus, for the frequency ω_0 and the quality factor Q

$$\omega_0 = \frac{\sqrt{I_{01}I_{02}}}{\sqrt{C_1C_2}V_T} \tag{54}$$

and

$$Q = \sqrt{\frac{C_2}{C_1}}\frac{\sqrt{I_{01}I_{02}}}{I_d} \tag{55}$$

with $I_{02} = I_{03}$. Observe that ω_0 and Q can be tuned orthogonally.

[At this point, it may be useful to note that the application of the analysis method described in Section IV to the circuit illustrated in Fig. 5 would confirm that the realized transfer function is indeed a second-order lowpass filter with parameters defined by (54) and (55).]

Other higher order transfer function synthesis examples, created by means of the proposed approach, can be found in [31].

VI. Simulation Results

The validity of the Bernoulli-cell approach was confirmed via indicative HSPICE simulations with process parameters from a commercial 1-GHz bipolar technology. No particular attempt was made to optimize the performance of the proposed circuits. This discussion concentrates on presenting results that are in close agreement with the theoretically predicted behavior. Although alternating current (ac) (small-signal) simulations are shown, the large-signal operation of the log-domain structures has been confirmed with large-signal multitone transient simulations since, for ac analysis, the simulator replaces each active device with its small-signal equivalent locally linearized around a direct current (dc) operating point. All simulations were carried out with the power-supply voltage set equal to 3.3 V.

A. Analysis Example

For the analysis example, the validity of (21)–(24) was verified. Setting arbitrarily $C_1 = C_2 = C = 5$ pF, $I_0 = I_{d1} = I_{d2} = 5\ \mu A$ and altering the current I_q, the dc gain varies according to (24) [see Fig. 7(a)], whereas a capacitator sweep verified the tuning of ω_0, according to (22), for an arbitrary value $I_q = 1\ \mu A$ [see Fig. 7(b)]. Similar confirming results were produced for other arbitrary values of currents and capacitors.

B. Synthesis Example

The transfer function of the lowpass filter synthesized in Section V reveals that when the currents I_{01}, I_{02} (with $I_{02} = I_{03}$) are varied in such a way that their product remains constant, then the transfer function (41) should remain unaltered. This observation raises the vital question of the optimum combination of currents when a particular filter is implemented. This paper does not aim to provide an answer to this question and concentrates only on presenting simulation results which confirm the validity of the proposed approach. An investigation of the best combination of currents for a particular desired frequency response is addressed in [29] where the case of a bandpass filter is elaborated. In practice, the relative magnitude of the dc bias currents will affect performance criteria, such as distortion and signal-to-noise ratio and, to the best of our knowledge, a thorough theoretical treatment of such criteria has yet to be presented for log-domain circuits. However, the proposed low-level method provides the designer with the freedom to conveniently experiment in achieving the design criteria, since various design objectives, such as ω_0 and Q, are related to the products of the biasing currents in a clear way.

The ac response of the lowpass filter of Fig. 5 was simulated for different current settings, as shown in Fig. 8. The f_0 frequencies for the two filters of Fig. 8(a) and (b) were theoretically equal to 15.3 and 490 MHz, respectively. Observe that, for different values of I_{01}, I_{02}, I_{03} but with the product $I_{01}I_{02} =$ constant, the frequency responses remain largely unaltered, as predicted from (53) and (54). The filter operates in class-A with the input current having the form $I_{\text{in}} = D[1 + m\sin(\omega t)]$ and D is the dc-component of the input. The filter of Fig. 8(a) showed a maximum total harmonic distortion (THD) level of 0.3% when an input tone of 1 MHz, modulated by $m = 50\%$, was applied. A similar THD value was obtained for the filter of Fig. 8(b) at an input frequency of 10 MHz. Fig. 8(a) shows close agreement between simulated and predicted ideal response for a variety of current value combinations corresponding to the same transfer function. This is in agreement with earlier published results [5], [31] and is expected since the filtering action, in this case $f_0 = 15.3$ MHz, takes place well below the unity-gain frequency f_T of the transistors $f_0/f_T \cong 10^{-2}$. The filter of Fig. 8(b) was simulated for two different values of D, namely $D = 100\mu A$ and $D = 400\mu A$. Since the respective frequency responses do not differ significantly, only the case for $D = 100\mu A$

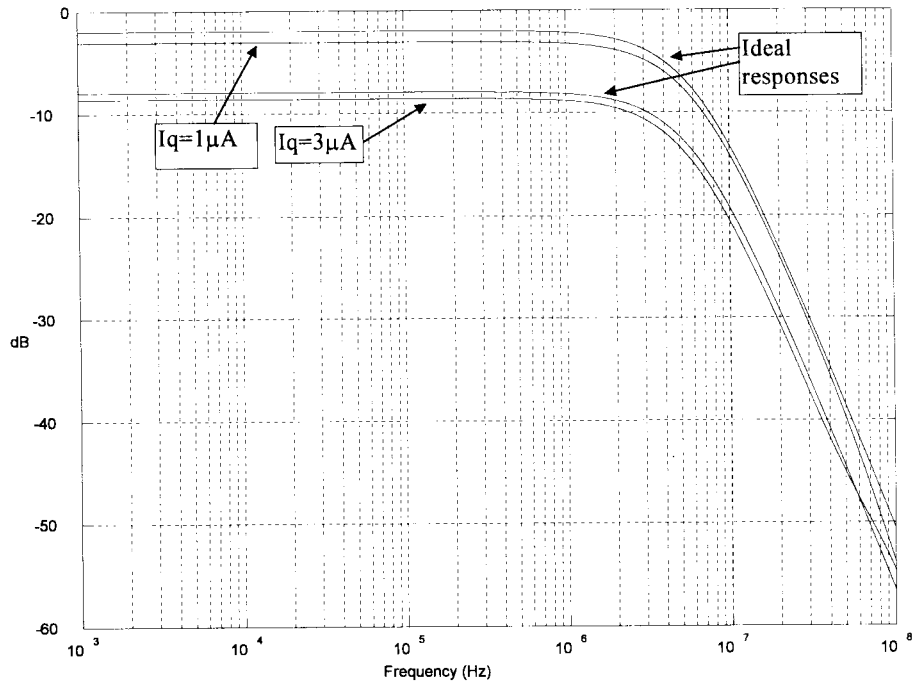

(a)

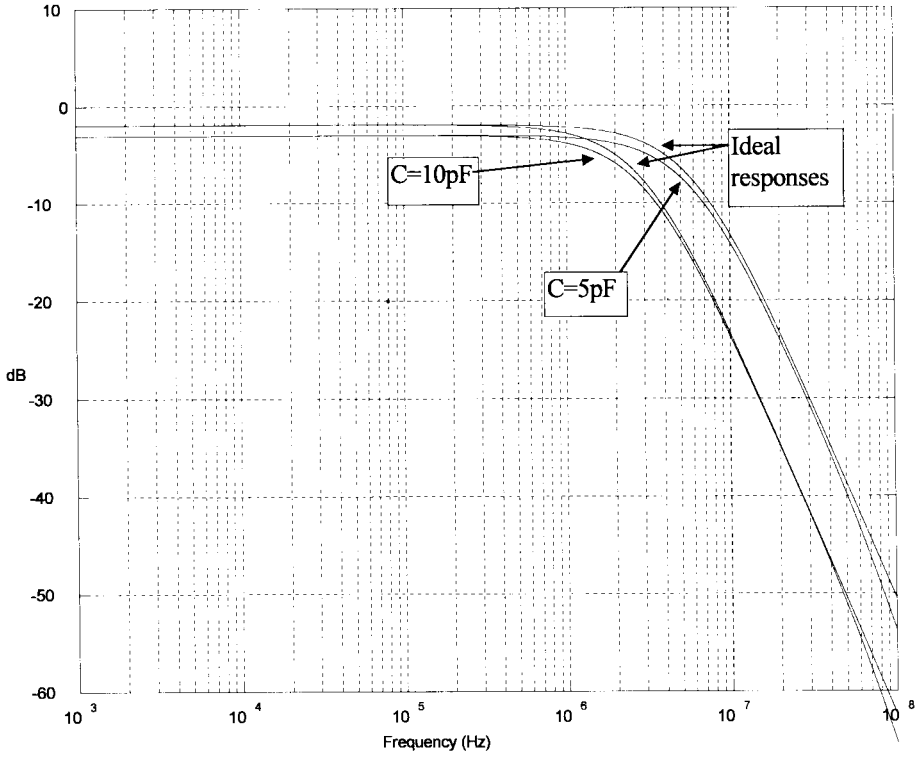

(b)

Fig. 7. Theoretical and simulated responses for the analysis example. (a) When I_q is varied. (b) When the capacitator is varied.

is shown in Fig. 8(b). However, when $D = 400\mu A$, i.e., when all the filter current values do not differ significantly, then input tones of the same frequency and modulation index m exhibit better linearity for high m values. In addition, at the expense of power consumption, high I_b values also lead to linearity improvement. In Fig. 8(b) there is a deviation between the simulated responses, which are close to each other as predicted, and the ideal response. This difference is due to the fact that the filtering ($f_0 = 490$ MHz) takes place at frequencies much closer to the f_T. In this case, the effect of the high-frequency parasitic poles is noticeable, causing peaking and altering the slope [32]–[34]. The simulated responses were confirmed by means of large $(m = 50\%)$ multitone transient simulations within an accuracy of $\cong 2$ dBs.

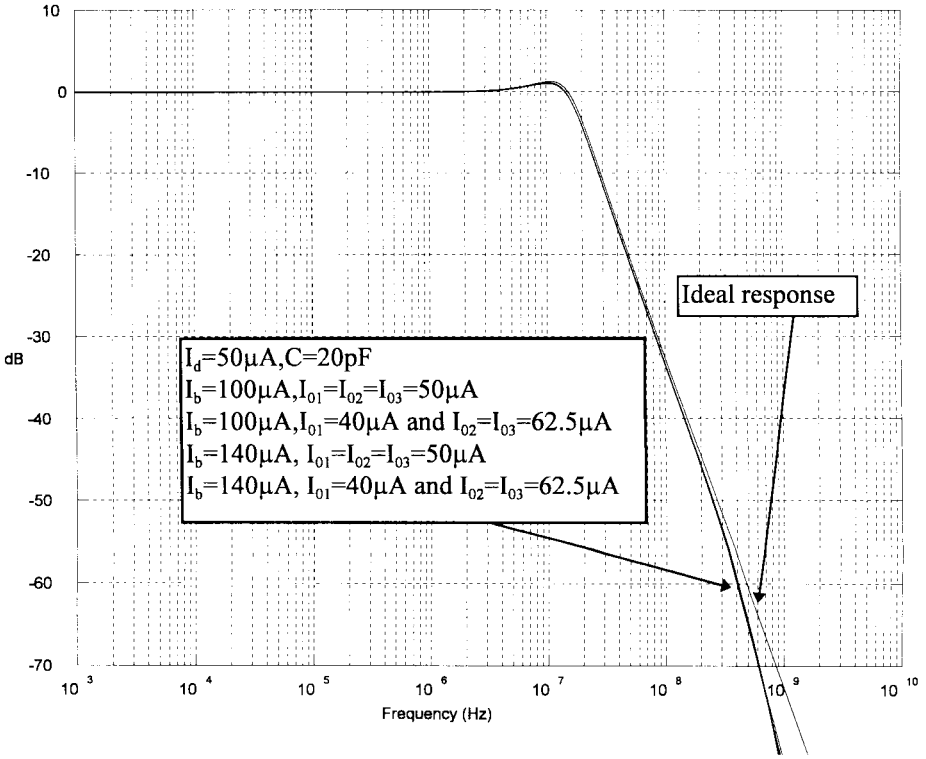

(a)

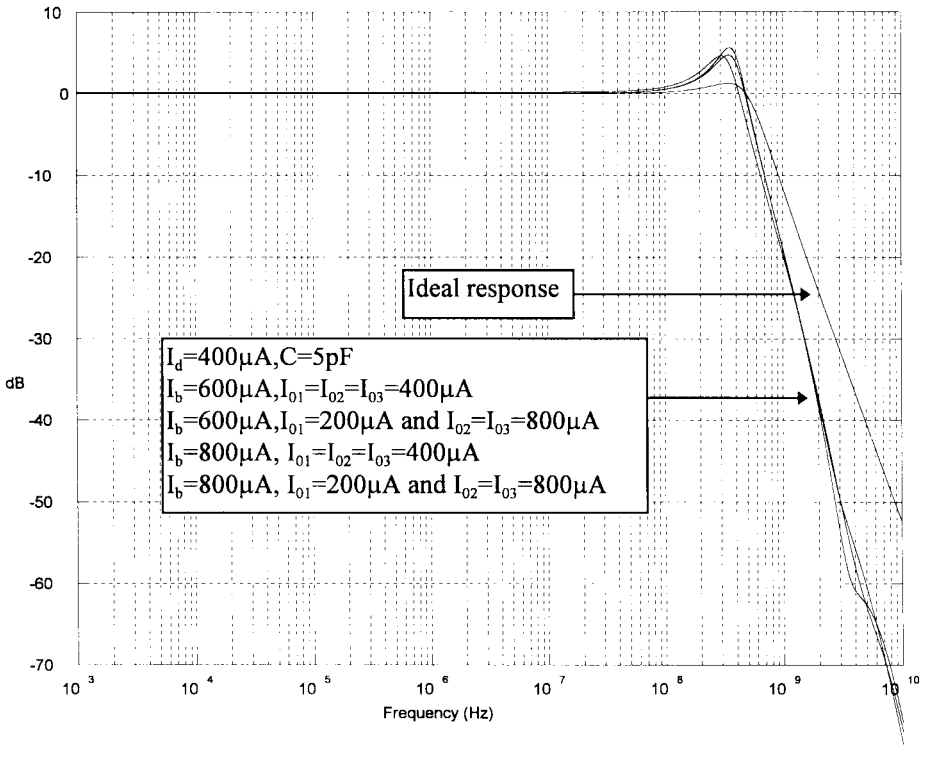

(b)

Fig. 8. Theoretical and simulated responses for the lowpass biquad. (a) When $f_0 = 15.3$ MHz. (b) When $f_0 = 490$ MHz.

VII. Conclusion

This paper has introduced a transistor-level nonlinear building block, termed a Bernoulli cell, and has described the application of this cell to the analysis and synthesis of log-domain structures. A low-level synthesis procedure is presented which does not require any high-level mapping and which reveals the relationships between high-level filter specifications and low-level circuit parameters in a clear way. These relationships offer the designer a degree of design flexibility to optimize the circuit-level implementation. As an analysis tool, the

Bernoulli-cell approach allows the designer to easily write down a set of transformed KCL equations describing the dynamic response of the internal currents, and hence derive an expression for the input–output transfer function. It is hoped that this alternative approach to log-domain circuit design may provide further insight into this new and promising class of circuits.

ACKNOWLEDGMENT

The authors would like to thank Ericsson Microelectronic Research Centre (MERC) for sponsoring this work, and the unknown reviewers for their fruitful suggestions which significantly improved the readability of this paper.

REFERENCES

[1] B. Gilbert, "Translinear circuits: A proposed classification," *Electron. Lett.*, vol. 11, no. 1, pp. 14–16, 1975.
[2] E. Seevink, "Analysis and synthesis of translinear integrated circuits," in *Studies in Electrical & Electronic Engineering 31*. Amsterdam, The Netherlands: Elsevier, 1988.
[3] B. Gilbert and E. Seevink Eds., "Translinear circuits," *J. Analog Integr. Circuits Signal Processing*, vol. 9, no. 2, 1996.
[4] R. W. Adams, "Filtering in the log-domain," presented at the 63rd AES Conf., New York, 1979.
[5] D. R. Frey, "Log-domain filtering: An approach to current-mode filtering," *Proc. Inst. Elect. Eng., G*, vol. 140, pp. 406–416, 1993.
[6] D. R. Frey, "Exponential state space filters: A generic current mode design strategy," *IEEE Trans. Circuits Syst. I*, vol. 43, pp. 34–42, Jan. 1996.
[7] Y. Tsividis, "Externally linear, time-invariant systems and their application to companding signal processors," *IEEE Trans. Circuits Syst. II*, vol. 44, pp. 65–85, Feb. 1997.
[8] E. Seevinck, "Companding Current-mode Integrator: A new circuit principle for continuous-time monolithic filters," *Electron. Lett.*, vol. 26, no. 24, pp. 2046–2047, 1990.
[9] Y. Tsividis, "On linear integrators and differentiators using instantaneous companding," *IEEE Trans. Circuits Syst. II*, vol. 42, pp. 561–564, Aug. 1995.
[10] Y. Tsividis, "General approach to signal processors employing companding," *Electron. Lett.*, vol. 31, no. 18, pp. 1549–1550, 1995.
[11] Y. Tsividis, "Instantaneously companding integrators," in *Proc. IEEE Int. Symp. Circuits Syst. (ISCAS'97)*, Hong-Kong, 1997, vol. I, pp. 477–480.
[12] D. R. Frey, "A 3.3 V electronically tuneable active filter useable to beyond 1 GHz," in *Proc. IEEE Int. Symp. Circuits Syst. (ISCAS'94)*, London, U.K., 1994, vol. 5, pp. 493–496.
[13] D. R. Frey, "On log-domain filtering for RF applications," *IEEE J. Solid-State Circuits*, vol. 31, pp. 1468–1475, Oct. 1996.
[14] D. R. Frey, "An adaptive analog notch filter using log-filtering," in *Proc. IEEE Int. Symp. Circuits Syst. (ISCAS'96)*, Atlanta, GA, 1996, vol. 1, pp. 297–300.
[15] F. Yang, C. Enz, and G. Ruymbeke, "Design of low-power and low-voltage log-domain filters," in *Proc. IEEE Int. Symp. Circuits Syst. (ISCAS'96)*, Atlanta, GA, 1996, vol. 1, pp. 117–120.
[16] C. Toumazou, J. Ngarnmil, and T. S. Lande, "Micro-power log-domain filter for electronic cochlea," *Electron. Lett.*, vol. 30, no. 22, pp. 1839–1841, 1994.
[17] M. Punzenberger and C. Enz, "A New 1.2 V BiCMOS log-domain integrator for companding current mode filters," in *Proc. IEEE Int. Symp. Circuits Syst. (ISCAS'96)*, Atlanta, GA, 1996, vol. 1, pp. 125–128.
[18] C. Enz, M. Punzenberger, and D. Python, "Low-voltage log-domain signal processing in CMOS and BiCMOS," in *Proc. IEEE Int. Symp. Circuits Syst. (ISCAS'97)*, Hong-Kong, 1997, vol. I, pp. 489–492.
[19] J. Mulder, W. A. Serdijn, A. C. van der Woerd, and A. H. M. van Roermund, "Signal x noise intermodulation in translinear filters," *Electron. Lett.*, vol. 33, no. 14, pp. 1205–1207, 1997.
[20] M. Punzenberger and C. Enz, "Noise in instantaneous companding filters," in *Proc. IEEE Int. Symp. Circuits Syst. (ISCAS'97)*, Hong-Kong, 1997, vol. 1, pp. 337–340.
[21] D. Perry and G. W. Roberts, "Log-domain filters based on LC ladder synthesis," in *Proc. IEEE Int. Symp. Circuits Syst. (ISCAS'95)*, Seattle, WA, 1995, pp. 311–314.
[22] J. Mulder, A. C. van der Woerd, W. A. Serdijn, and A. H. M. van Roermund, "General current-mode analysis method for translinear filters," *IEEE Trans. Circuits Syst. I*, vol. 44, pp. 193–197, Mar. 1997.
[23] M. Punzenberger and C. Enz, "Low-voltage companding current-mode integrators," in *Proc. IEEE Int. Symp. Circuits Syst. (ISCAS'95)*, Seattle, WA, 1995, pp. 2112–2115.
[24] E. Kreyszig, *Advanced Engineering Mathematics*. New York: Wiley, 1962.
[25] G. Stephenson and P. M. Radmore, *Advanced Mathematical Methods for Engineering and Science Students*. Cambridge: Cambridge Univ. Press, 1980.
[26] K. A. Stroud, *Engineering Mathematics*. London, U.K.: Macmillan, 1995.
[27] E. Drazin, *Non-Linear Systems*. Cambridge: Cambridge Univ. Press, 1992.
[28] E. M. Drakakis, A. J. Payne, and C. Toumazou, "Bernoulli operator: A low-level approach to log-domain processing," *Electron. Lett.*, vol. 33, no. 12, pp. 1008–1009, 1997.
[29] E. M. Drakakis, A. J. Payne, and C. Toumazou, "Log-domain state-space: A systematic transistor-level approach for log-domain filtering," *IEEE Trans. Circuits Syst. II*, Mar. 1999.
[30] K. Lokere, "Log-domain continuous time integrated filters," M.S. thesis, Katholieke Univ. Leuven, Leuven, Belgium and Imperial College, London, London, U.K., 1996.
[31] E. M. Drakakis, A. J. Payne, and C. Toumazou, "Log-domain filters, translinear circuits and the Bernoulli cell," in *Proc. IEEE Int. Symp. Circuits Syst. (ISCAS'97)*, Hong-Kong, 1997, vol. I, pp. 501–504.
[32] H. Khorramabadi and P. R. Gray, "High-frequency CMOS continuous-time filters," *IEEE J. Solid-State Circuits*, vol. 19, pp. 939–948, Jun. 1984.
[33] V. Copinathan, Y. P. Tsividis, K.-S. Tan, and R. K. Hester, "Design considerations for high-frequency continuous-time filters and implementation of an antialiasing filter for digital video," *IEEE J. Solid-State Circuits*, vol. 25, pp. 1562–1574, 1990.
[34] S. D. Willingham and K. Martin, *Integrated Video-Frequency Continuous-Time Filters—High Performance Realizations in BiCMOS*. Norwell, MA: Kluwer, 1995.

Emmanuel Michael Drakakis received the B.Sc. degree in physics and the M.Phil. in electronic physics from Aristotle University of Thessaloniki, Macedonia, Greece, in 1991 and 1994, respectively.

In 1996 he was a Research Associate at the Greek State Army Research and Technology Centre, Electronics and Physics Division. Since 1996 he has been studying for the Ph.D. degree in the Department of Electrical Engineering, Imperial College, London, U.K. His main research interests include device modeling, circuit theory, bio-inspired systems, and the design of high-frequency robust analog integrated circuits.

Mr. Drakakis was awarded Performance Scholarships from the Foundation of State Scholarships in 1986 and 1988.

Alison J. Payne (S'90–M'95) received the B.Eng. and Ph.D. degrees from the Imperial College of Science, Technology and Medicine, London, U.K., in 1989 and 1992, respectively.

From 1992 to 1994 she worked as a Design Engineer for GEC-Plessey Semiconductors, Swindon, U.K., where she was involved in the design of analog integrated circuits for radiopaging receivers, with particular emphasis on low-voltage and low-power operations. She is currently a Lecturer in Analog Circuit Design in the Department of Electrical and Electronic Engineering, Imperial College. Her research interests include RF bipolar and CMOS analog circuit design, fully integrated analog filters, robust analog design, and circuit synthesis methodologies. She has published various papers in international journals and conferences in the field of analog IC design.

Dr. Payne is currently Vice President of the IEEE Circuits and Systems (U.K. Chapter) Committee and is also President-Elect of the IEEE Circuits and Systems Society Analog Signal Processing Technical Committee.

Chris Toumazou (M'87) received the B.Sc. degree in engineering and the Ph.D. in electrical engineering from Oxford-Brookes University, Oxford, U.K., in 1983 and 1986 respectively.

He is currently the Mahanakorn Professor of Analog Circuit Design in the Department of Electrical and Electronic Engineering, Imperial College, London, U.K. His research interests include high-frequency analogue integrated circuit design in bipolar, CMOS and GaAs technology and low power electronics for biomedical applications. He has authored or coauthored over 200 publications in the field of analog electronics.

Dr. Toumazou is a member of the Analog Signal Processing Committee of the IEEE Circuits and Systems Chapter, for which he served as Chariman from 1992 to 1994, and is also a committee member of the Circuits and Systems Chapter of the U.K. and Republic of Ireland Section of the IEEE. He is a past Associate Editor of the IEEE TRANSACTIONS ON CIRCUITS AND SYSTEMS and is an Editor for the *IEE Electronics Letters*. He is currently Vice-President for Technical Activities for the IEEE Circuits and Systems Society and is also a Life Member of the Electronics Society of Thailand. He is cowinner of the IEE 1991 Rayleigh Best Book Award. He is also recipient of the 1992 IEEE Circuits and Systems Society Outstanding Young Author Award as well as cowinner of the 1995 IEE Electronics Letters Best Paper Premium.